Chemical Engineering Journal 524 (2025) 167911

Contents lists available at ScienceDirect

Chemical Engineering Journal

journal homepage: www.elsevier.com/locate/cej

Enhancing onboard carbon capture performance by tailored absorbents and process optimization: Insights from pilot-scale testing and simulation

Chengjin Pan [a], Zhicheng Wu [a], Zhengang Zhou [a], Lingyu Shao [e,*], Junjie Zheng [a], Can Zhou [a], Haitao Shen [b], Haidong Fan [c], Shihan Zhang [e], Chenghang Zheng [a,c,d,**], Xiang Gao [a,c,d,**]

[a] State Key Lab of Clean Energy Utilization, State Environmental Protection Engineering Center for Coal-Fired Air Pollution Control, Zhejiang University, Hangzhou 310027, PR China
[b] Zhejiang Energy Marine Environmental Technology Co., LTD., Hangzhou 311200, PR China
[c] Baima Lake Laboratory (Zhejiang Provincial Laboratory of Energy and Carbon Neutrality), Hangzhou 310051, PR China
[d] Key Laboratory of Clean Energy and Carbon Neutrality of Zhejiang Province, Jiaxing Research Institute, Zhejiang University, Jiaxing 314000, PR China
[e] Science and Education Integration College of Energy and Carbon Neutralization, Zhejiang University of Technology, Hangzhou 310014, PR China

ARTICLE INFO

Keywords:
Onboard carbon capture system
Marine sector decarbonization
Absorbent optimization
Waste heat recovery
Regeneration heat consumption

ABSTRACT

Maritime CO_2 emissions account for approximately 3 % of global emissions and continue to rise with the growth of international trade, underscoring the urgent need for onboard carbon capture system (OCCS) technologies. However, OCCS deployment faces challenges, including limited installation space, high flue gas velocity, and low CO_2 partial pressure, which collectively reduce capture efficiency and elevate energy demand. In this study, an Aspen Plus rate-based model was employed to determine absorber dimensions and key operating parameters through sensitivity analysis. The optimized configuration was implemented in a 1.2 MW pilot platform for validation under ship-like exhaust conditions. Among the tested solvents, the polyamine-based SWCS-3 solvent significantly enhanced absorption performance, achieving a steady-state capture efficiency of 90.6 %, while reducing regeneration energy consumption by 31.5 % compared with monoethanolamine (MEA). The integration of waste heat recovery (WHR) process reduced regeneration heat consumption by 14.4 %, while the further incorporation of rich solvent split (RSS) and lean vapor recompression (LVR) modifications reduced the requirement to 2.66 GJ/t CO_2. Overall, the results demonstrate that the proposed OCCS can achieve high CO_2 capture efficiency within stringent marine constraints, providing a pathway toward the decarbonization of maritime transport.

1. Introduction

Maritime shipping accounts for over 80 % of global trade by volume, playing a pivotal role in international trade and global supply chains [1]. However, the maritime sector faces significant challenges in achieving decarbonization. According to the International Maritime Organization (IMO), the maritime industry emits approximately 1056 million tons of CO_2 annually, accounting for 3 % of global emissions. With the continuous growth of global maritime trade, CO_2 emissions from shipping are projected to increase by 50 % by 2050 compared to 2018 levels [2]. Alternative fuels, such as liquefied natural gas, methanol, and hybrid technologies, show promise but remain in the early stages of adoption, with over 90 % of the current fleet continuing to rely on fossil fuels [3]. In response to the escalating urgency of climate change, the IMO has adopted increasingly stringent regulations and standards, targeting a reduction of at least 20 % in annual greenhouse gas emissions by 2030 and aiming for achieving near-zero emissions around 2050 [4].

In the long term, fuel substitution offers an attractive path toward reducing carbon emissions in the maritime sector [5]. However, the transition to cleaner fuels faces significant barriers, including the construction of novel infrastructure, the slow renewal of the global fleet, and uncertainty surrounding future fuels, resulting in substantially higher expenses [6]. In contrast, onboard carbon capture system (OCCS) provides a more practical mid-term solution to shipping decarbonization, with advantages including lower retrofitting costs, minimal disruption to existing systems, and compatibility with existing vessels

* Corresponding author.
** Corresponding authors at: State Key Lab of Clean Energy Utilization, Zhejiang University, Hangzhou 310027, PR China.
E-mail addresses: slyaimer014@zjut.edu.cn (L. Shao), zhengch2003@zju.edu.cn (C. Zheng), xgao1@zju.edu.cn (X. Gao).

https://doi.org/10.1016/j.cej.2025.167911
Received 9 July 2025; Received in revised form 28 August 2025; Accepted 30 August 2025
Available online 2 September 2025

[7]. The CO_2 concentration in emissions from marine diesel engines typically ranges from 4 to 6 vol%, classifying it as a low-concentration point source (<15 vol%) [8]. Chemical absorption, in which CO_2 reacts with absorbent to form chemical compound and releases CO_2 upon heating, stands out as a mature and scalable technology [9]. It is especially suitable for handling large volumes of flue gas with low CO_2 concentrations, making it one of the most promising pathways for OCCS [10]. Achieving effective CO_2 capture from ship exhaust lies in the selection of appropriate absorbents and process configurations that can ensure high CO_2 absorption efficiency while minimizing regeneration heat consumption [11]. In addition, OCCS also faces challenges that extend beyond absorption performance alone. Factors such as equipment size constraints, system integration compatibility, operational safety, and cost must also be carefully considered to ensure practical deployment on marine vessels [12].

Chemical absorbents primarily include amines, ammonia, inorganic salts, amino acid salts, and ionic liquids. Among these, amines, especially monoethanolamine (MEA), are the most extensively studied and widely employed [13]. Primary and secondary amines like MEA and Diethylenetriamine (DETA) typically exhibit high CO_2 absorption efficiency, but with relatively high regeneration energy requirements due to the formation of stable carbamate species [14]. In contrast, tertiary amines like *N*-methyldiethanolamine (MDEA) facilitate CO_2 hydration to form bicarbonate, which is easier to desorb but suffers from lower absorption rates. In recent years, specially structured amines such as piperazine (PZ), morpholine (MOR), and 2-amino-2-methyl-1-propanol (AMP) have attracted increasing attention due to their unique performance characteristics [15,16]. Yu et al. [17] demonstrated that MOR exhibits a lower pH than MEA due to its six-membered heterocyclic structure, promoting the formation of fewer carbamate and more bicarbonate during CO_2 absorption. Moreover, the lower viscosity of MOR enhances mass transfer, contributing to improved CO_2 absorption efficiency. To overcome the limitations of single-component amines, blended amine systems have been developed to integrate the strengths of different solvents [18]. Zhang et al. [19] investigated a ternary mixture of MEA/MDEA/PZ, which showed higher CO_2 absorption efficiency and lower regeneration energy consumption. Technologies for low-concentration CO_2 capture have been extensively implemented in land industrial applications, such as post-combustion capture from coal-fired flue gases [20]. However, the CO_2 concentration in marine exhaust is even lower, posing stricter requirements on the absorption rate of the solvent. As a result, absorbents with relatively slow kinetics have limited potential for OCCS applications [21]. Furthermore, spatial constraints in the engine room limit the size of equipment such as absorber. Solvents like biphasic absorbents and ionic liquids, which typically exhibit high viscosities, may hinder mass transfer and increase operational complexity [22,23]. Their application requires careful evaluation.

Several research institutions have investigated OCCS technologies. Luo et al. [24] developed an integrated model of ship energy system coupled with CO_2 capture system. Their findings indicated that, due to limited thermal and electrical energy available on board, the maximum achievable CO_2 capture rate was restricted to 73 %, with an estimated cost of approximately €77.50/t CO_2. Increasing the capture rate to 90 % by installing an additional diesel generator would raise the capture cost by 1.1 times, mainly due to the extra fuel consumption. Feenstra et al. [25] examined the integration of exhaust heat with the reboiler of the stripper in a diesel-powered vessel, reporting a total cost of capture and liquefaction of about €98/t CO_2 at a 90 % capture rate. Lee et al. [26] developed a CO_2 capture system using Aspen Plus for an 18.2 MW cargo vessel, employing a 22 wt% MDEA +8 wt% PZ solvent. The reboiler energy consumption was reported to be 3.27 GJ/t CO_2. Most of these studies focus on simulation, with solvent selection and process configuration largely relying on experience derived from land-based industrial applications. However, pilot-scale validation studies and detailed investigations on operational strategies for OCCS remain scarce in the existing literature. Therefore, further in-depth research on onboard CO_2 capture systems is necessary.

Considering the inherent complexity and operational constraints of shipboard environments, the deployment of efficient, low-energy-demand absorbents, coupled with carefully designed process configurations and optimized operating parameters, is critical for achieving effective onboard CO_2 capture. In this work, we propose a comprehensive strategy that includes absorbent formulation optimization and integration of energy-saving processes, aiming to enhance CO_2 capture performance, reduce energy demand, and improve the adaptability of onboard systems. The performance of a polyamine-promoted solvent with enhanced mass transfer properties was evaluated on a pilot-scale platform. A steady-state process model was developed using Aspen Plus and validated against pilot data. Furthermore, the effectiveness of integrating ship exhaust heat recovery to reduce regeneration energy was assessed. These efforts aim to provide a practical, compact, and energy-efficient pathway to improve the feasibility of OCCS and to accelerate the decarbonization of the maritime sector.

2. Design and parameter optimization of onboard carbon capture system

OCCS faces unique challenges due to limited engine room space and stringent maritime safety regulations, necessitating compact equipment designs, particularly for absorbers in terms of both column diameter and height [27]. Meanwhile, according to the vapor–liquid equilibrium (VLE) of amine-based CO_2 absorption, the low CO_2 partial pressure in ship exhaust leads to a lower CO_2 loading of the rich solvent, which adversely impacts the efficiency of regeneration and increases energy consumption (Supplementary Fig. S1). Therefore, it is essential to implement strategies that mitigate these drawbacks, thereby enhancing the economic feasibility of OCCS.

2.1. Process modeling

The Aspen Plus Rate-based modeling framework is widely recognized as a reliable tool for the design and optimization of amine-based CO_2 capture processes, as evidenced by its extensive application in large-scale post-combustion capture projects. It considers the phase equilibrium, reaction equilibrium, and reaction kinetics at the mass transfer interface. It also incorporates chemical reaction enhancement factors and corrections for effective interfacial area, providing a more accurate estimation of gas-liquid mass transfer compared to the equilibrium model [28]. By discretizing the mass and heat transfer processes across individual column stages, the model enables detailed prediction of both thermodynamic and kinetic parameters within the absorption column. Although onboard operating environments feature unique constraints, the underlying gas–liquid absorption mechanisms remain consistent with those of land-based CO_2 capture systems. By incorporating marine-specific exhaust properties, spatial limitations, and operational constraints into the simulation, the Aspen Plus model can reliably represent OCCS performance.

To accurately account for the significant effects of ion–molecule interactions on the CO_2 absorption–desorption process, the electrolyte non-random two-liquid (*E*-NRTL) model was employed to predict the gas-liquid phase equilibrium. This model is particularly suitable for representing the phase behavior of multi-component electrolyte systems [29]. The thermodynamic properties of the PZ-MEA-CO_2-H_2O system were obtained from the NIST chemical database and the amines property package in Aspen Plus. Reaction parameters for the PZ-MDEA-CO_2-H_2O system can be referred in our previous work [30]. Supplementary Table S1 summarizes the equilibrium reactions and equilibrium constants (K_{eq}), which were calculated using Eq. (1). Supplementary Table S2 lists the kinetically controlled reactions along with their activation energies and pre-exponential factors. The kinetic expressions were modeled using the power-law equation shown in Eq. (2).

$$\ln K_{eq} = A + \frac{B}{T} + ClnT + DT \quad (1)$$

$$Kinetic\ factor = ke^{-E/RT} \quad (2)$$

Fig. S2 illustrates the developed simulation model for the absorption and desorption of CO_2 from ship exhaust gas. The flue gas composition was set based on typical exhaust from marine diesel engines [31], with appropriate exhaust components simplifications made that do not affect the simulation accuracy for CO_2 capture [32]. Under baseline conditions, the standardized volumetric flow rate of the flue gas was 3500 Nm^3/h, with a composition of 6.0 vol% CO_2, 7.6 vol% H_2O, 13.7 vol% O_2, and 72.7 vol% N_2.

In the OCCS, the absorber is the largest single piece of equipment, and its dimensions must comply with engine room space constraints. The superficial gas velocity (u) in the absorber was calculated as Eq. (3).

$$u = Q_g \Big/ \left(3600 \bullet \frac{\pi D^2}{4}\right) \quad (3)$$

where Q_g is the flow rate of the gas, m^3/h; and D is the absorber diameter, m.

The packing height H_p was determined from Eq. (4).

$$H_p = HTU \times NTU \quad (4)$$

where HTU represents the packing height required to achieve a single transfer unit of mass transfer, and NTU represents the number of such units required to achieve the target removal efficiency. Both HTU and NTU can be estimated using empirical correlations based on gas–liquid properties, packing type, and operating conditions, and can also be calculated within the Aspen Plus rate-based design framework. To meet the target CO_2 capture efficiency of >80 % while accounting for space constraints, the absorber diameter was set at 0.96 m under the baseline conditions, corresponding to a superficial gas velocity of 1.54 m/s, with a packing height of 6.0 m (Supplementary Note 1). Based on this configuration, a sensitivity analysis of key design parameters was conducted.

2.2. Sensitivity analysis

Fig. 1 (a) illustrates the effect of absorber packing height on CO_2 capture efficiency and regeneration heat consumption using a 30 wt% MEA solvent. When the column packing height was reduced from 8.0 m to 3.0 m, the CO_2 capture efficiency decreased by 6.5 %, while the regeneration heat consumption increased from 5.17 GJ/t CO_2 to 5.47 GJ/t CO_2, representing a 5.5 % increase. The lower column height shortened the residence time of the absorbent, hindering CO_2 mass transfer. Similarly, reducing the absorber diameter increases the flue gas velocity, and its impact on CO_2 absorption performance is shown in Fig. 1 (b). As the velocity increased from 0.63 m/s to 2.10 m/s, CO_2 capture efficiency decreased by 3.6 %, while the regeneration heat consumption rose from 5.14 GJ/t CO_2 to 5.29 GJ/t CO_2. Higher flue gas velocities reduce the gas–liquid contact time, impeding CO_2 absorption.

The impact of different absorbent formulations on CO_2 capture performance was also investigated. Fig. 1 (c) depicts the CO_2 cyclic capacity for three solutions: 30 wt% MEA, 10 wt% PZ + 20 wt% MDEA, and 5 wt% PZ +25 wt% MEA. For each formulation, the minimum regeneration heat consumption and the corresponding CO_2 cyclic capacity were selected for comparison. The addition of 5 wt% PZ to the MEA solution increased the rich loading by 0.03 mol CO_2/mol amine. In

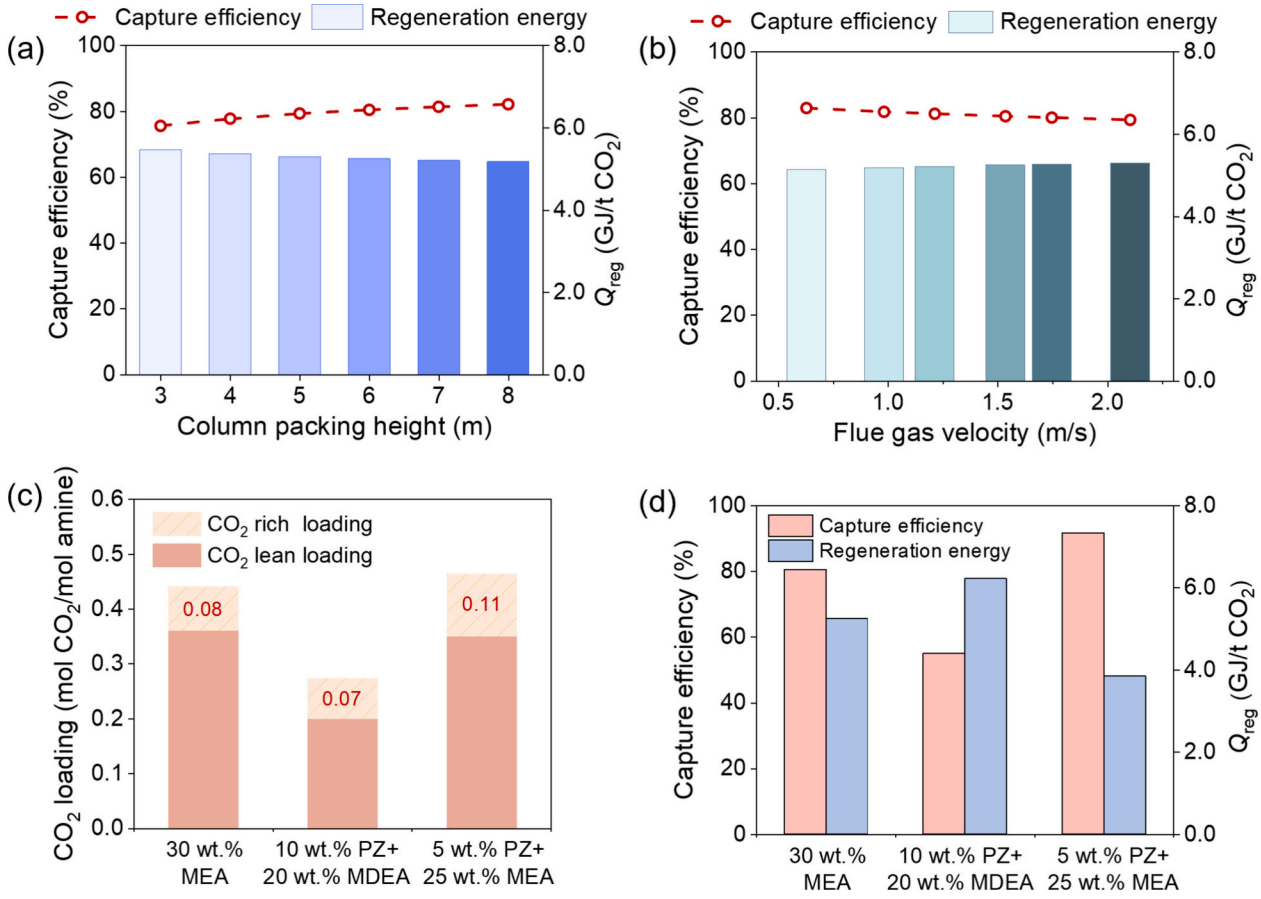

Fig. 1. Effect of (a) absorber column packing height and (b) flue gas velocity on CO_2 capture efficiency and regeneration heat consumption (Q_{reg}). (c) CO_2 loading and (d) CO_2 capture efficiency and Q_{reg} with different absorbents.

contrast, the PZ/MDEA blend, which used tertiary amine as the main absorbent, exhibited the lowest rich loading among the three absorbents. As shown in Fig. 1 (d), the PZ/MEA blend demonstrated the highest CO_2 capture efficiency, reaching 91.66 %. It also exhibited the lowest regeneration heat consumption at 3.85 GJ/t CO_2, representing a 26.7 % reduction compared to MEA alone. Conversely, the PZ/MDEA blend showed the lowest capture efficiency of only 55.06 %, and the highest regeneration heat consumption of 6.22 GJ/t CO_2. These results demonstrate that tertiary amines, despite their low regeneration energy potential, are unsuitable under onboard conditions due to inherently slow reaction kinetics. Similarly, conventional monoamines fall short in delivering sufficient capacity and kinetics. In contrast, polyamines such as PZ offer faster absorption kinetics and higher CO_2 loading, making them highly suitable for maritime applications [33]. To further reduce energy consumption, the integration of energy-saving processes is essential. Based on these insights, an optimized CO_2 capture strategy for ship exhaust was developed, combining advanced absorbent formulations with energy-saving process modifications (Supplementary Fig.S3).

The preceding sensitivity analysis quantitatively elucidated the effects of absorber dimensions and solvent selection on CO_2 capture performance under marine operating conditions. Based on these findings, the column geometry was determined to meet both spatial constraints and the target capture efficiency. By integrating the preliminary Aspen Plus design results with reference data from other large-scale amine-based CO_2 capture plants [34,35], a complete set of design parameters was established, as summarized in Table 1. These parameters provided the engineering basis for the design and construction of the 1.2 MW marine diesel engine flue gas carbon capture platform described in Section 3.

3. Pilot platform and experimental methods

3.1. Chemicals

DETA (99.5 %, BASF Co., Ltd., China), PZ (99.8 %, Delamine Co., Ltd., The Netherlands), and MOR (99.5 %, BASF Co., Ltd., China) were utilized to prepare an aqueous SWCS-3 solutions of 30 wt% (DETA: PZ: MOR = 1:1:4). MEA (99 %, BASF Co., Ltd., China) was used to prepare an aqueous solution of 30 wt% MEA. All solutions were prepared using deionized water. The above chemicals were directly used without additional purification.

3.2. Experimental and analytical methods

The schematic diagram and physical image of the ship exhaust CO_2 capture platform are shown in Fig. 2. The pilot system consists of a pre-scrubbing tower, an absorber and a stripper. A 1.2 MW marine diesel engine set (Supplementary Table S3) was used as the exhaust gas source, providing a maximum treatment capacity of approximately 6000 Nm^3/h. The detailed exhaust gas composition and flow rates under different load conditions are summarized in Supplementary Table S2. The high-temperature exhaust gas, initially at 280–300 °C, was purified and cooled to 40–50 °C before being introduced into the absorber. The absorber is 15.0 m tall with a diameter of 0.96 m and a packing height of 6.0 m. In absorber, the absorbent and flue gas were brought into counter-current contact to absorb CO_2, then the CO_2-rich solvent was sent to the stripper after passing through the heat exchanger. The stripper has a height of 9.3 m, a diameter of 0.64 m, and a packing height of 2.0 m. The heat required for desorbing CO_2 was supplied by the steam generated from a fuel oil-fired boiler. The regenerated high-temperature lean solvent was subsequently cooled and recirculated to the absorber, while the desorbed gas was condensed and pass through a gas-liquid separator to obtain CO_2 product gas. Two liquid sampling points were installed after rich liquid pump and lean liquid pump, respectively. Additionally, two DN25 gas sampling points were positioned at the inlet and outlet of the absorber.

Table 1
Main operating parameters of onboard CO_2 capture process.

Part	Parameter	Unit	Value
Pre-scrubber	Column height	m	3.0
	Column diameter	m	0.96
Absorber	Packing height	m	6.0
	Liquid-to-gas ratio	L/m^3	3–7
	Column diameter	m	0.96
	Packing	/	Mellapak 250Y
Heat exchanger	Logarithmic mean temperature difference	°C	10
Stripper	Pressure	kPa	201
	Packing height	m	2.0
	Column diameter	m	0.64
	Packing	/	Mellapak 250Y
	Reboiler temperature	°C	119.15

The Total Organic Carbon Analyzer (TOC-L CPN, Shimadzu Corporation, Japan, ± 4 μg/L) was employed to measure the CO_2 loading in liquid samples. The pH of the solution was measured using a pH electrode (HC3800, HACH Ltd., US, ± 0.1 pH). A non-dispersive infrared multi-gas analyzer (MGA5, MRU Ltd., Germany, ± 0.01 vol%) was used to measure the CO_2 concentration. To prevent condensation of water and amine vapors, the sampling probe and line were heated to 150 °C and 120 °C, respectively. The CO_2 capture efficiency was calculated using Eq. (5):

$$\eta = \frac{y_{in} - y_{out}}{y_{in}} \times 100\% \quad (5)$$

where y_{in} and y_{out} denote the CO_2 concentrations at the absorber inlet and outlet, respectively.

The regeneration heat consumption of the CO_2 desorption process was calculated based on the enthalpy and mass flow rate of the vapor entering and leaving the reboiler, as described in Eq. (6):

$$Q_{reg} = \frac{\dot{m}_{steam} h_{steam} - \dot{m}_{cond} h_{cond}}{\dot{m}_{CO_2} \times 10^3} \quad (6)$$

where $\dot{m}_{steam}$ and $\dot{m}_{cond}$ are the mass flow rates of steam entering and condensate exiting the reboiler, kg/h, respectively; h_{steam} and h_{cond} are the specific enthalpy of steam and condensate, kJ/kg, respectively; and $\dot{m}_{CO_2}$ is the mass flow rate of CO_2 product gas, kg/h.

4. Results and discussion

4.1. Pilot-scale validation of CO_2 capture performance on a 1.2 MW marine diesel engine exhaust system

4.1.1. CO_2 capture performance using MEA and SWCS-3 solutions

To evaluate the performance of OCCS under unique constraints of onboard applications, a pilot-scale test platform was established with the exhaust from a 1.2 MW marine diesel engine, and long-term continuous operation experiments were conducted. The CO_2 capture performance of MEA and SWCS-3 solutions was investigated from system startup to steady-state operation, at a flue gas flow rate of 3500 m^3/h and a liquid-to-gas (L/G) ratio of 4 L/m^3, as shown in Fig. 3 (a) and (b). In contrast, the SWCS-3 solution achieved an initial capture efficiency exceeding 95 % and was able to maintain 64.7 % efficiency after 30 min. It should be noted that the observed decrease in CO_2 capture efficiency during the initial period corresponds to the start-up phase when the reboiler was intentionally kept off. This operational strategy was adopted to allow the solvent to approach near-saturation before regeneration starts, thereby shortening the transition time to steady-state absorption–desorption balance. Consequently, the initial lean CO_2

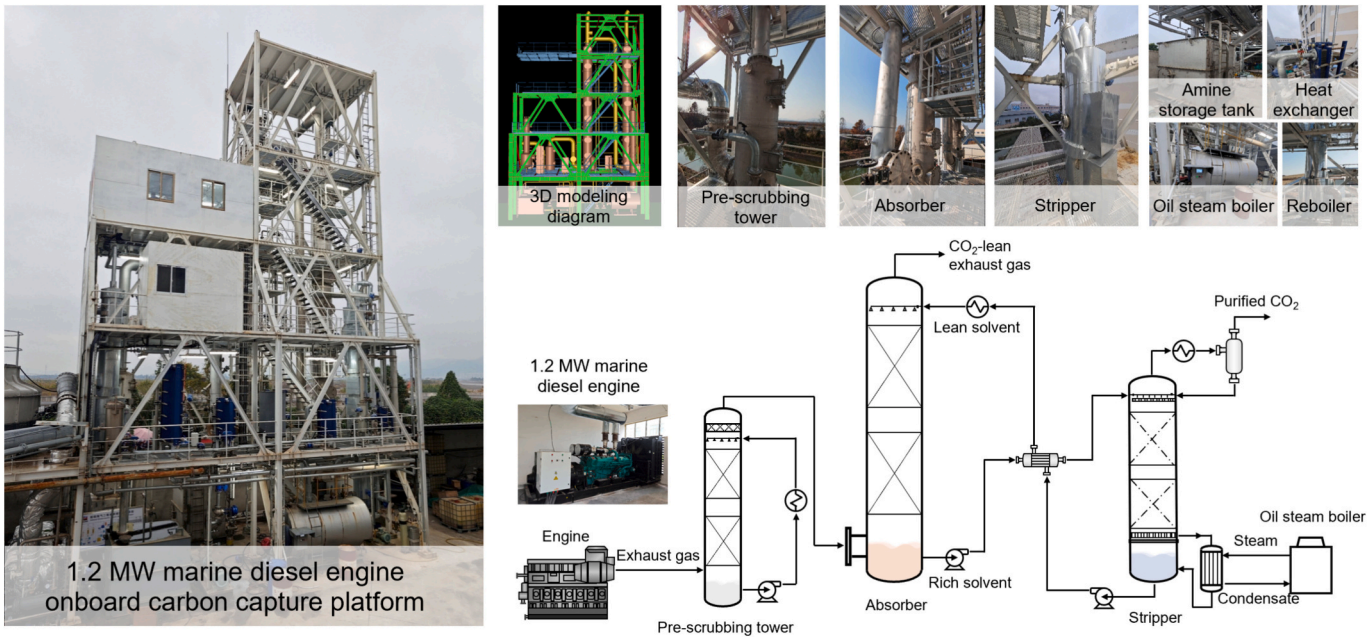

Fig. 2. Schematic and image of ship exhaust gas CO_2 capture platform.

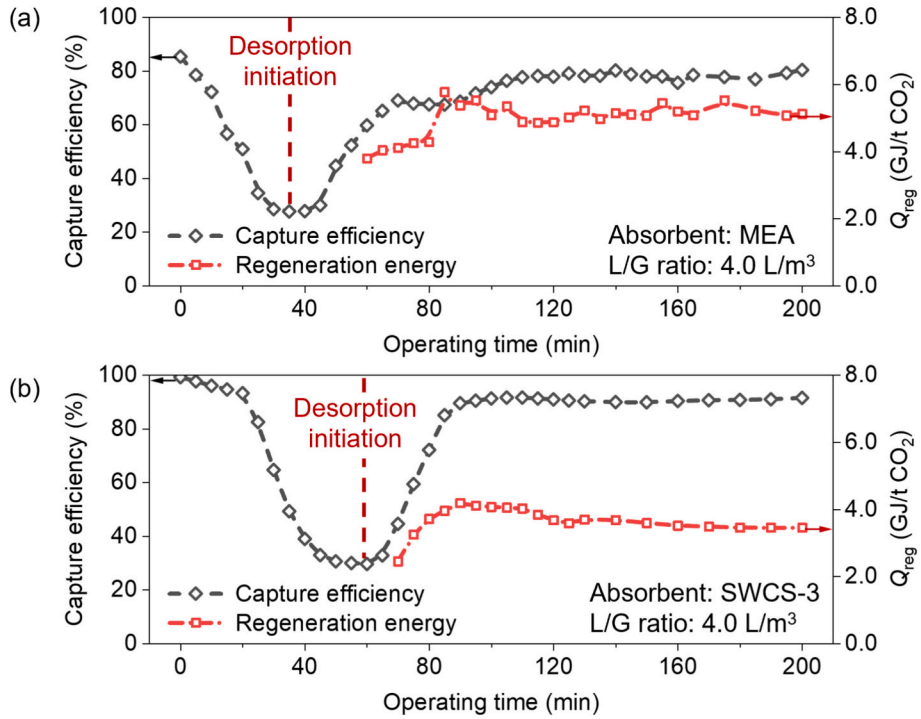

Fig. 3. Change in CO_2 capture efficiency and Q_{reg} over a 200-min long-term experiment using (a) MEA and (b) SWCS-3 solutions.

loading was low, resulting in a temporarily high driving force and capture efficiency, which declined as the solvent became progressively saturated. For the MEA solution, the capture efficiency initially reached 85.3 % but dropped sharply to 28.5 % within 30 min. Saturation was not reached until approximately 50 min, resulting in a desorption start time around 20 min later. Compared to the single-component MEA, SWCS-3, which formulated with polyamines such as PZ and DETA, showed significantly enhanced absorption kinetics and CO_2 loading capacity under low CO_2 partial pressure conditions.

The CO_2 loading and pH values of lean and rich solvents after the initiation of desorption were analyzed, as shown in Fig. 4. Since the reboiler required time to reach its operating temperature, regeneration heat consumption was not measured during the initial heating period, and data collection began only after a stable CO_2 flow was established. Fig. 4 (a) illustrates the variation in CO_2 loading and pH over time for the MEA solvent. After 40 min, the CO_2 loading of the MEA solution reached 0.52 mol CO_2/mol amine. Following the onset of desorption, the CO_2 loadings of both rich and lean solvents gradually decreased, accompanied by an increase in pH. During the initial absorption-only period, the solvent approached gas–liquid equilibrium with high CO_2 loading, which contributed to relatively low regeneration heat consumption. As the absorption–desorption circulation progressed, the rich

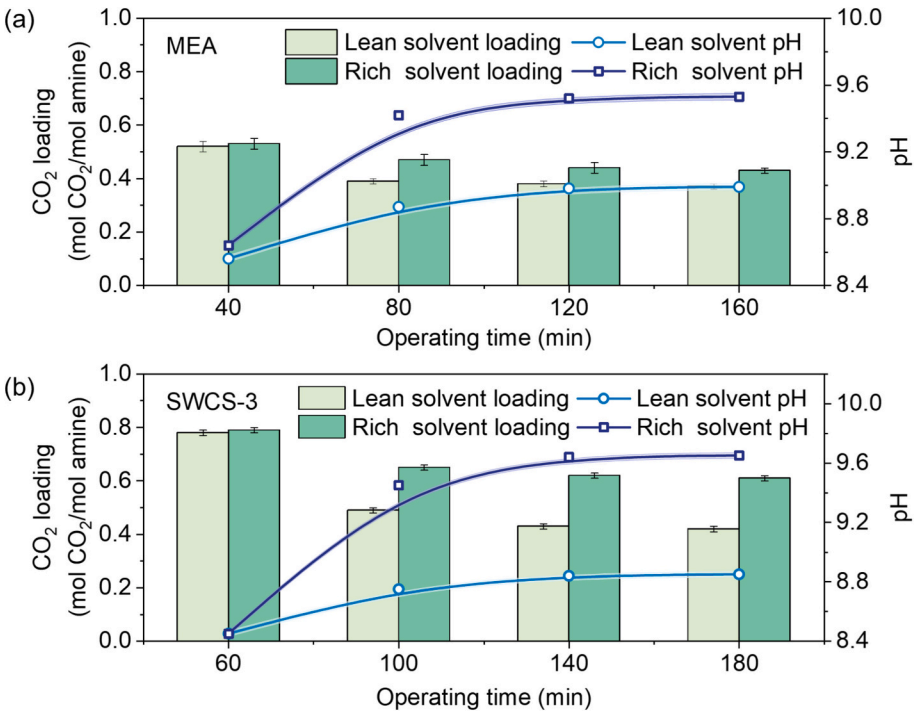

Fig. 4. Change in CO_2 loading and pH of lean and rich solvents over a 200-min long-term experiment using (a) MEA and (b) SWCS-3 solutions.

loading steadily decreased, leading to an increase in regeneration heat consumption. This decline was primarily attributed to mass transfer limitations caused by high flue gas velocity and low CO_2 partial pressure, which hindered the solvent from reaching its full absorption capacity. At the steady state reached after 160 min, the CO_2 loadings of the rich and lean solvents were 0.45 and 0.38 mol CO_2/mol amine, respectively, resulting in a cyclic capacity of only 0.07 mol/mol. The corresponding pH values were 8.99 and 9.53.

Fig. 4 (b) presents the performance of the SWCS-3 solution over time. After 60 min of operation, the rich loading reached 0.78 mol CO_2/mol amine, with a corresponding pH of 8.45. The system reached steady state until 130 min, with rich and lean loadings of 0.59 and 0.41 mol CO_2/mol amine, respectively, corresponding to a cyclic capacity of 0.18 mol CO_2/mol amine. This value was 1.57 times higher than that of the MEA solution. The pH values of the rich and lean solvents were 8.85 and 9.65, respectively. At steady state, the MEA solution achieved an average CO_2 capture efficiency of 80.3 % and a regeneration heat consumption of 5.04 GJ/t CO_2. In contrast, the SWCS-3 solution reached steady-state operation faster and exhibited a higher average capture efficiency of 90.6 %, along with a significantly lower regeneration heat consumption of 3.45 GJ/t CO_2, representing a 31.5 % reduction compared to MEA. These experimental results confirm that the incorporation of polyamines effectively improves the performance of amine-based absorbents under challenging conditions involving high flue gas velocity and low CO_2 partial pressure.

During the 72-h cyclic operation of the SWCS-3 solution, samples were periodically collected to monitor its compositional stability. Under relatively constant liquid levels in the absorber, stripper, and circulation tanks, the relative total nitrogen concentration (c_{TN}) of the absorbent gradually decreased with operating time, showing a reduction of approximately 1.6 % after 72 h (Supplementary Fig. S4), primarily attributed to solvent volatilization during the absorption–desorption process. The corresponding loss was less than 1 kg/t CO_2, demonstrating the good stability of the SWCS-3. It is worth noting that black carbon carried in the marine diesel exhaust continuously accumulated in the absorbent, leading to a gradual darkening of the solvent color (Supplementary Fig. S5). Although no significant effects on capture efficiency or energy consumption were observed in this experiment, the enrichment of oil-like substances may pose a potential risk to the long-term operational stability of the system.

Fig. 5 compares the experimental and simulated results for CO_2 capture efficiency and regeneration heat consumption under steady-state conditions. Under identical lean loading and L/G ratio conditions, the simulated capture efficiency for the MEA solution was slightly higher than the experiment, with a relative error of 3.49 %. The simulated regeneration heat consumption was 5.19 GJ/t CO_2, representing a 2.98 % increase compared to the experiments. These results fall within the acceptable experimental error range, confirming the reliability of the simulation model. Minor deviations may be attributed to fluctuations in pump flow rate and reboiler temperature during the experimental operation. Due to the absence of reliable reaction and interaction parameters for DETA, MOR with CO_2 in the Aspen Plus database, a PZ/MEA blended solvent was used as a substitute for the SWCS-3 solution in the simulation. The simulated CO_2 capture efficiency was 88.7 %, which was 2.10 % lower than the experimental value, while the simulated regeneration heat consumption was 3.71 GJ/t CO_2, 7.54 % higher than the experimental measurement. These findings suggest that the PZ/MEA can serve as a reasonable proxy for SWCS-3 in predictive modeling, which is critical for subsequent process optimization. Nevertheless, the superior performance of the SWCS-3 solution compared to the PZ/MEA blend should not be overlooked.

4.1.2. *Effect of exhaust gas flow rates on CO_2 capture performance*

Under the experimental conditions described previously, the effect of exhaust gas flow rate on the CO_2 absorption performance of the SWCS-3 solution was investigated. The flow rate was regulated by adjusting the engine load of the marine diesel generator. As shown in Fig. 6 (a), when the engine operated at 25 % load, the exhaust gas flow rate reached approximately 2500 Nm^3/h. Under this condition, the CO_2 capture efficiency reached 91.8 %, representing a 1.2 % increase compared to the result at 3500 Nm^3/h. The regeneration heat consumption decreased by 0.6 %. As the exhaust gas flow rate increased, the gas velocity within the absorber also increased, resulting in reduced gas–liquid contact time and diminished CO_2 rich loading, which led to higher regeneration heat

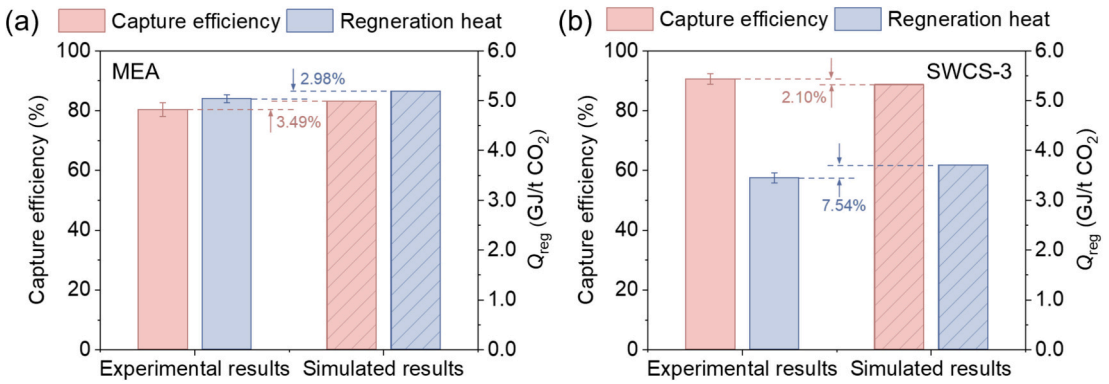

Fig. 5. Comparison of experimental and simulated results for CO_2 capture efficiency and Q_{reg} using (a) MEA and (b) SWCS-3 at 4.0 L/m^3.

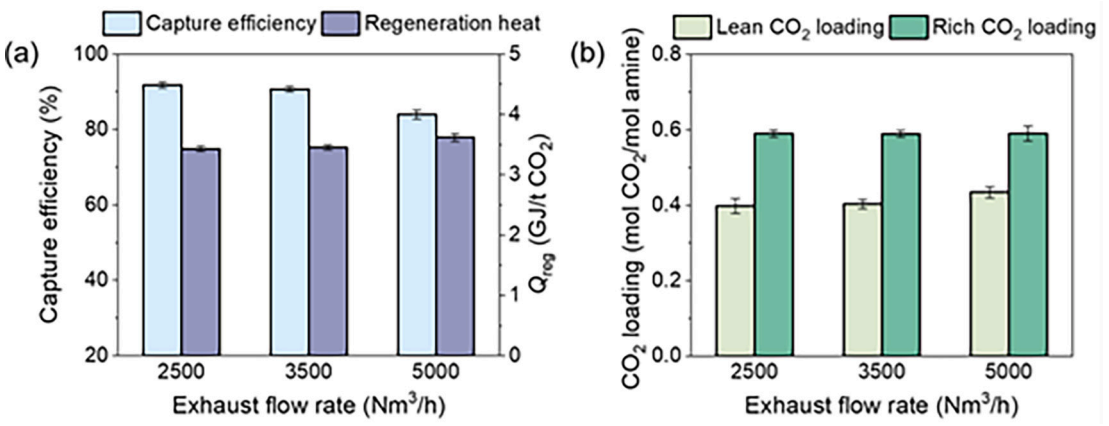

Fig. 6. Effect of exhaust gas flow rate on (a) CO_2 capture efficiency and Q_{reg}, and (b) CO_2 loading of lean and rich solvent.

consumption, as illustrated in Fig. 6 (b). At an exhaust gas flow rate of 5000 Nm^3/h, the gas velocity within the absorber column increased to approximately 2 m/s. Under the high-velocity conditions, the CO_2 capture efficiency dropped significantly to 84.0 %, representing a 6.6 % decrease compared to the result at 3500 Nm^3/h. Concurrently, the regeneration heat consumption rose to 3.62 GJ/t CO_2, marking a 4.7 % increase.

4.1.3. *Effect of L/G ratio on CO_2 capture performance*

To address the high gas velocity condition of >2 m/s encountered in ship diesel exhaust, the effect of L/G ratio adjustments on CO_2 capture efficiency, cyclic capacity, and regeneration heat consumption was investigated, as shown in Fig. 7 (a) and (b). Increasing the L/G ratio can enhance capture efficiency, but a higher liquid flow will also reduce the residence time. This increased the mass transfer gradient, which consequently lower the rate of CO_2 accumulation in the rich solvent. As the L/G ratio increased from 4.0 to 5.0 L/m^3, the CO_2 capture efficiency rose to 85.0 %. However, the cyclic capacity decreased from 0.15 to 0.13 mol CO_2/mol amine, leading to an increase in regeneration heat consumption to 3.74 GJ/t CO_2. Notably, further increasing the L/G ratio to 6.0 L/m^3 resulted in a decline in capture efficiency. This was primarily due to the excessive liquid holdup within the packing, which caused localized flooding and impaired the gas-liquid mass transfer. Under this condition, the cyclic capacity dropped to 0.10 mol CO_2/mol

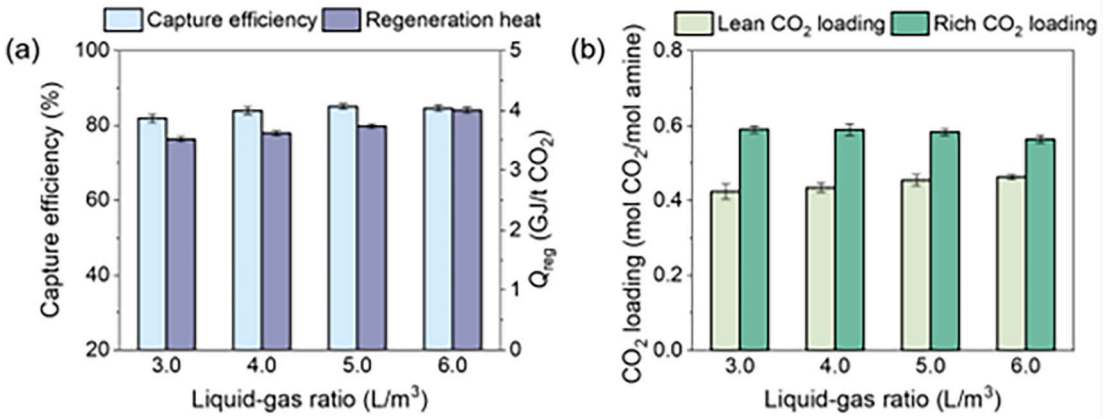

Fig. 7. Effect of L/G ratio on (a) CO_2 capture efficiency and Q_{reg}, and (b) CO_2 loading of lean and rich solvent.

amine, and regeneration heat consumption increased to 4.05 GJ/t CO_2. Conversely, reducing the L/G ratio to 3.0 L/m^3 yielded a capture efficiency of 81.8 %, with a lower regeneration heat consumption of 3.52 GJ/t CO_2. Given the inherently low CO_2 partial pressure in marine exhaust gas, maintaining high capture efficiency negatively impact energy demand. A moderate reduction in L/G can enhance solvent regeneration, achieving both a higher cyclic capacity and reduced regeneration energy consumption, while maintaining the target CO_2 capture efficiency. This optimization is particularly beneficial in ship-based applications, where minimizing solvent inventory and system weight is crucial under stringent space constraints. Therefore, if ultra-high capture efficiency is not required, a properly reduced L/G ratio is

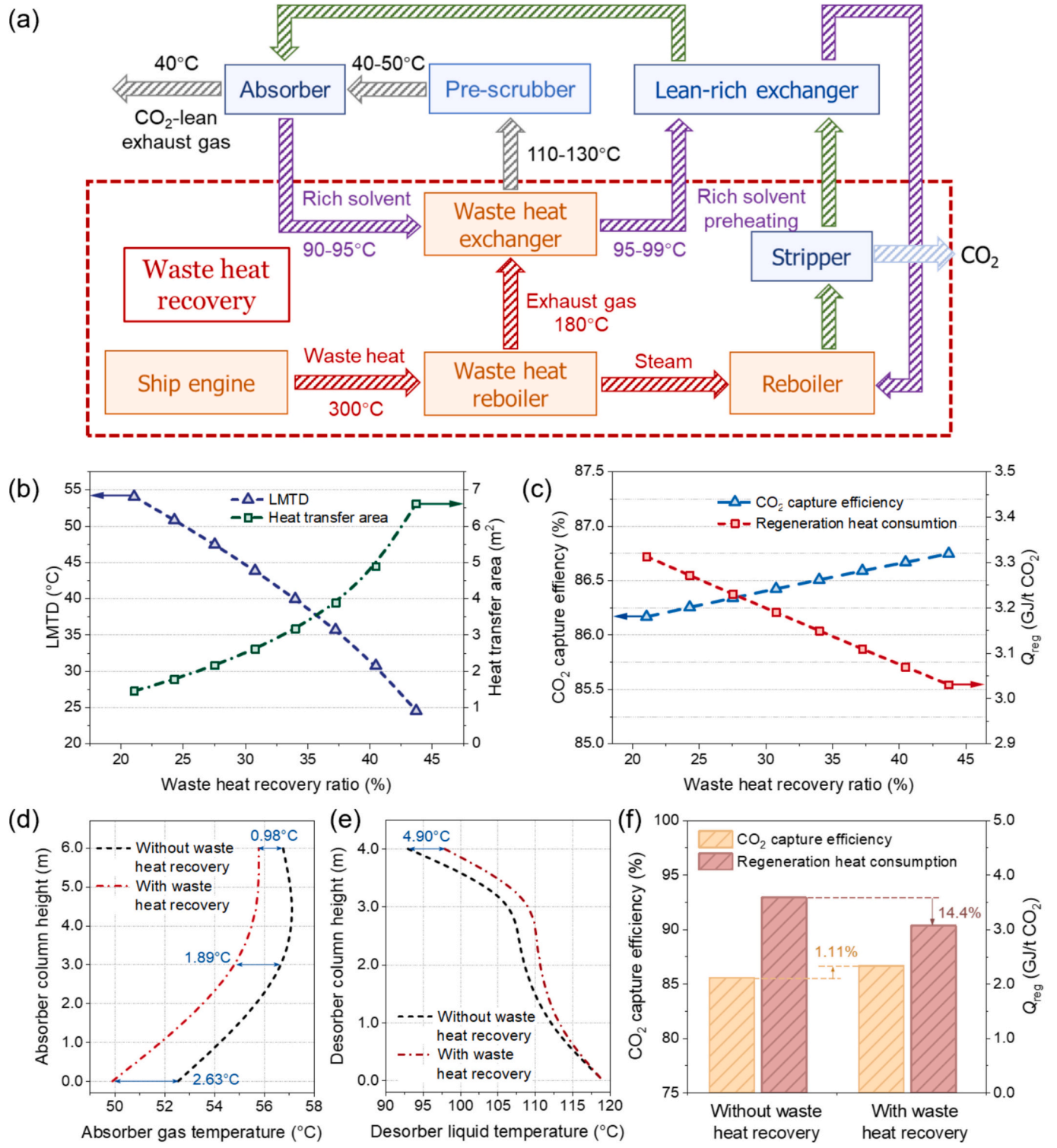

Fig. 8. (a) Schematic diagram of the modified ship exhaust gas CO_2 capture system modification incorporating waste heat recovery (WHR). (b) Optimized unit design and (c) improved capture performance of the WHR exchanger under different WHR ratios. Temperature distribution changes in the (d) absorber gas phase and (e) stripper liquid phase resulting from the WHR modification. (f) Overall optimization effect of applying WHR process. All results presented are based on process simulation.

recommended to balance energy performance with operational stability.

4.2. Process optimization of onboard carbon capture system

4.2.1. Integration of exhaust waste heat recovery in OCCS

Both experimental and simulation results confirmed that optimizing the absorbent formulation can improve CO_2 capture efficiency and reduce regeneration energy consumption. However, there remains further potential for further energy savings. Marine diesel engines typically emit high-temperature exhaust gas, for instance, the 1.2 MW diesel engine used in the pilot platform generated exhaust temperature up to 280–300 °C. However, to ensure effective CO_2 absorption, the inlet flue gas temperature of must be maintained at 40–50 °C, requiring a substantial amount of cooling water This not only causes substantial thermal energy loss but also increases space demands for cooling equipment. To address this, a process modification leveraging waste heat recovery (WHR) was proposed, utilizing the sensible heat of exhaust gas to improve the thermal efficiency of the desorption process. Since part of the exhaust heat was used by the waste heat boiler to generate steam, the boiler outlet temperature (180 °C in this study) was adopted as the effective initial temperature for WHR calculations. Given the relatively small variation in the specific heat capacity of the exhaust gas, the waste heat utilization efficiency (η_{heat}) was calculated using Eq. (7):

$$\eta_{heat} = \frac{t_{initial} - t_{final}}{t_{initial} - t_{ambient}} \times 100\% \quad (7)$$

where $t_{initial}$ represents the available initial temperature, which in this work is taken as the exhaust temperature at the outlet of the waste heat boiler, 180 °C, t_{final} is the exhaust temperature after passing through the heat recovery exchanger, $t_{ambient}$ is the ambient temperature, which is assumed to be 25 °C.

Fig. 8 (a) presents the proposed process flow diagram. A gas-liquid heat exchanger was installed upstream of the pre-scrubber to preheat the rich solvent using high-temperature exhaust gas, thereby reducing the thermal load on the reboiler. Cooling the exhaust gas before the absorber also improves CO_2 absorption and reduces cooling water consumption. To balance energy efficiency with the compact design requirements of onboard systems, a target WHR ratio of 20 % to 45 % of the theoretical recoverable thermal load was selected. Since that the primary heat transfer resistance in gas–liquid exchangers lie on the gas side, the overall heat transfer coefficient was set to an average of 450 W/(m^2·K) based on phase-change considerations.

As shown in Fig. 8 (b), increasing the WHR ratio leads to a larger heat transfer area and a lower logarithmic mean temperature difference (LMTD). This trade-off is critical in determining the optimal recovery rate, as a lower LMTD improves thermal efficiency but necessitates larger equipment. Fig. 8 (c) illustrates the effects of different recovery ratios on CO_2 capture efficiency and regeneration heat consumption. As the exhaust gas temperature decreased from 147.3 °C to 112.2 °C, the WHR ratio increased from 21.1 % to 43.7 %, resulting in a 0.57 % increase in capture efficiency and an 8.46 % decrease in regeneration heat consumption, from 3.31 to 3.03 GJ/t CO_2. However, in practical engineering applications, excessively high recovery ratios may cause minimal temperature differentials at the heat exchange interface, posing challenges in exchanger size and cost. Therefore, a recovery ratio of 40.5 % was selected, corresponding to a heat exchange area of 4.88 m^2 and an LMTD of 30.7 °C.

To comprehensively evaluate the impact of the WHR process on the thermal distribution within the absorber and stripper columns, a comparative analysis was conducted before and after the integration of the WHR process. Fig. 8 (d) illustrates the temperature profile of the absorber gas phase. Following the implementation of the WHR modification, the gas temperature entering the absorber decreased from 52.55 °C to 49.92 °C. Due to the intense gas-liquid reactions occurring in the upper section of the column, a peak was observed in the middle section, reaching 55.79 °C, which represents a reduction of 1.89 °C compared to the conventional process. This reduction in gas phase temperature mitigated the heat release associated with the exothermic CO_2 absorption reaction, thereby enhancing CO_2 loading of the rich solvent [36]. Fig. 8 (e) depicts the temperature profile of the liquid phase within the stripper. The results show that preheating the rich solvent using waste heat increased its temperature from 93.00 °C to 97.90 °C at the stripper inlet. The temperature gradient of the liquid phase gradually decreased along the downward flow of the rich solvent. The elevated inlet temperature of the rich solvent reduced the sensible heat required for regeneration, thus improving the thermal efficiency of the reboiler. As shown in Fig. 8 (f), as the WHR ratio was set as 40 %, the CO_2 capture efficiency increased by 1.11 % compared to the conventional process, while the regeneration heat consumption decreased to 3.07 GJ/t CO_2, representing a 14.4 % reduction. These results demonstrate that the WHR is a promising approach for enhancing the performance of OCCS.

4.2.2. Combined process modifications with rich solvent split and lean vapor recompression

The integration of multiple process modifications can further optimize the energy performance of CO_2 capture systems, producing a synergistic effect wherein the whole exceeds the sum of its parts [37]. Additional process modifications, including rich solvent split (RSS) [38] and lean vapor recompression (LVR) [39], were integrated into the ship exhaust CO_2 capture system to improve the energy demand of CO_2 desorption. The developed OCCS process incorporating energy-saving modifications is shown in Fig. 9 (a). Our previous studies on post-combustion CO_2 capture in power plants have demonstrated the energy-saving potential of RSS and LVR modifications [30]. The key parameters of these modifications were also detailly evaluated.

In the RSS modification, the rich solvent exiting the absorber was divided into two streams. The primary stream was sent through the lean-rich heat exchanger and then introduced into the middle position of stripper. Meanwhile, the other unheated rich solvent, was fed directly to the top of the stripper without heat exchange. This configuration enabled effective heat recovery from the high-temperature regeneration gas, thereby reducing the energy demand for CO_2 desorption [40]. The regeneration heat consumption was affected by the RSS ratio, which is defined as the ratio of the cold rich solvent flow rate to the hot rich solvent flow rate, as shown in supplementary Fig. S6. The minimum regeneration heat consumption was achieved when the split ratio was between 0.20 and 0.30. An excessively high split ratio resulted in an insufficient flow of rich solvent passing through the lean-rich heat exchanger, which prevented full recovery of the sensible heat from the regenerated hot lean solvent and ultimately increased the regeneration heat consumption. As illustrated in supplementary Fig. S7, when the split ratio was set to 0.20, the RSS modification increased the temperature gradient in the stripper. The introduction of cold rich solvent at the top of the stripper lowered the upper-column temperature, which increased the CO_2 partial pressure while decreasing the H_2O vapor partial pressure. This change reduced the latent heat required for water evaporation and lowered the condenser load. Meanwhile, the liquid-phase temperature in the middle section of the stripper increased, which facilitated CO_2 desorption.

The LVR process involved the addition of a flash tank to evaporate the high-temperature lean solvent discharged from the stripper. The resulting vapor was compressed by a mechanical compressor and subsequently reintroduced into the stripper, thereby facilitating internal heat recovery and improving thermal efficiency [41]. Since the LVR recovered the sensible heat of the hot lean solvent and reduced the lean solvent temperature entering the lean-rich heat exchanger, the combination of RSS and LVR was adopted as a common process optimization configuration, as the RSS process reduced the flow rate of rich solvent entering the lean-rich heat exchanger [42]. As shown in Fig. 9, the

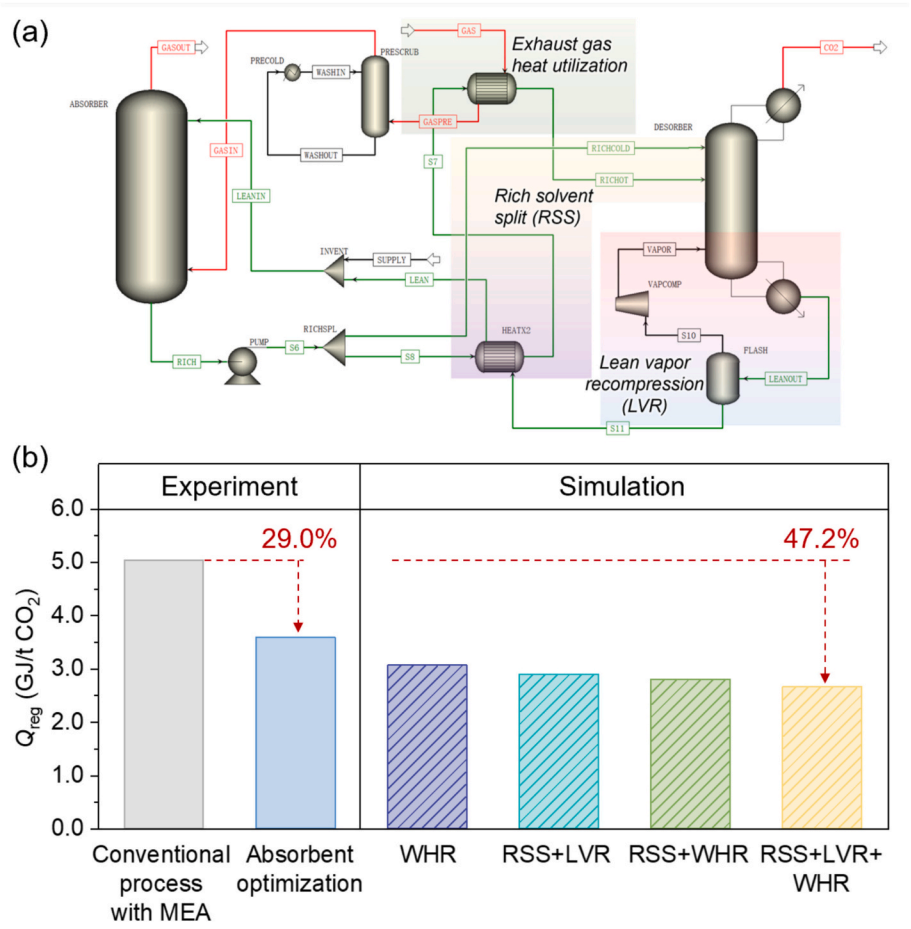

Fig. 9. (a) The developed OCCS process incorporating energy-saving modifications. (b) Q_{reg} of the selected energy-saving process configurations.

combined RSS + LVR configuration, with a RSS ratio of 0.20 and a flash pressure of 1 bar, reduced regeneration heat consumption to 2.90 GJ/t CO_2, with the compressor power penalty included. When further coupled with WHR modification, the regeneration heat consumption decreased to 2.66 GJ/t CO_2, representing a 47.2 % reduction compared to the conventional process using MEA. Additionally, applying RSS in combination with WHR achieved a regeneration heat consumption of 2.80 GJ/t CO_2, exceeding the performance of the RSS + LVR configuration. This indicates that ships where LVR modification is impractical can still achieve considerable energy savings by adopting a hybrid approach with RSS and WHR. Although these process modifications have not yet been fully implemented in the pilot plant of this study, the same modeling methodology has been successfully applied and validated in our previous large-scale land-based CO_2 capture projects [41]. In these projects, strategies such as RSS, LVR, and WHR were implemented based on simulation analyses. The measured reductions in regeneration heat consumption closely matched the simulated predictions, supporting their potential applicability in OCCS.

5. Conclusion

In summary, our study demonstrated that OCCS are technically feasible under the challenging conditions of marine environments, including limited equipment space, high flue gas velocity, and low CO_2 concentration. To address these constraints, a rate-based Aspen Plus model was employed to conduct sensitivity analyses on absorber dimensions and operating parameters, ensuring that the final design satisfied both spatial limitations and capture efficiency requirements. The optimized configuration formed the basis for the construction of a 1.2 MW pilot platform, where experimental validation under ship-like exhaust conditions confirmed the system's performance. Among the tested solvents, the polyamine-promoted SWCS-3 solution achieved a 90.6 % steady-state capture efficiency with 31.5 % lower regeneration heat consumption compared to MEA. Process optimization further showed that adjusting the liquid-to-gas ratio can balance energy demand without significant loss of capture efficiency. To enhance energy efficiency, WHR modification was integrated, reducing regeneration heat consumption by 14.4 %, while additional process modifications (RSS and LVR) further decreased the energy requirement to 2.66 GJ/t CO_2, representing a 47.2 % reduction relative to the conventional MEA process. Despite these promising results, several practical challenges must still be overcome for large-scale deployment of OCCS, including increased system weight and energy demands, operation under dynamic sea conditions, limited onboard personnel, corrosion resistance, and the complexity of CO_2 compression, storage, and offloading logistics. Addressing these issues through compact, lightweight designs, robust automation, and optimized operating strategies will be essential for the successful integration of OCCS technologies into maritime decarbonization pathways. This work provides both experimental validation and process optimization insights, offering a practical roadmap toward efficient, compact, and energy-saving CO_2 capture solutions for the shipping industry.

CRediT authorship contribution statement

Chengjin Pan: Writing – original draft, Visualization, Validation, Methodology, Investigation, Formal analysis, Conceptualization. **Zhicheng Wu:** Validation, Methodology, Investigation, Data curation, Conceptualization. **Zhengang Zhou:** Investigation, Formal analysis, Data curation. **Lingyu Shao:** Methodology, Conceptualization. **Junjie**

Zheng: Methodology, Investigation. **Can Zhou:** Methodology, Investigation. **Haitao Shen:** Resources, Project administration. **Haidong Fan:** Supervision, Resources, Funding acquisition. **Shihan Zhang:** Methodology. **Chenghang Zheng:** Writing – review & editing, Validation, Supervision, Project administration, Methodology, Funding acquisition, Conceptualization. **Xiang Gao:** Validation, Supervision, Project administration, Methodology, Funding acquisition, Conceptualization.

Declaration of competing interest

The authors declare that they have no known competing financial interests or personal relationships that could have appeared to influence the work reported in this paper.

Acknowledgements

This work was supported by the Key R&D Program of Zhejiang Province (No. 2024SSYS0072), National Key Research and Development Program of China (No. 2022YFC3701500), "Pioneer" and "Leading Goose" R&D Program of Zhejiang (No. 2023C03156), and National Natural Science Foundation (No. 52500144).

Appendix A. Supplementary data

Supplementary data to this article can be found online at https://doi.org/10.1016/j.cej.2025.167911.

Data availability

Data will be made available on request.

References

[1] Y.-y. Lau, Q. Chen, M.C.-P. Poo, A.K.Y. Ng, C.C. Ying, Maritime transport resilience: a systematic literature review on the current state of the art, research agenda and future research directions, Ocean Coast. Manage. 251 (2024) 107086.
[2] IMO, Fourth IMO Greenhouse Gas Study 2020, 2020.
[3] UNCTAD, Review of Maritime Transport 2024, 2024.
[4] IMO, IMO Strategy on Reduction of GHG Emissions from Ships, 2023.
[5] P. Balcombe, J. Brierley, C. Lewis, L. Skatvedt, J. Speirs, A. Hawkes, I. Staffell, How to decarbonise international shipping: options for fuels, technologies and policies, Energ. Conver. Manage. 182 (2019) 72–88.
[6] B. Stolz, M. Held, G. Georges, K. Boulouchos, Techno-economic analysis of renewable fuels for ships carrying bulk cargo in Europe, nature Energy 7 (2022) 203–212.
[7] A. Kumar, P. Sridhar, S. Farooq, I.A. Karimi, Designing amine-based capture units onboard LNG-run ships, Industrial & Engineering Chemistry Research 63 (2024) 19600–19612.
[8] L. Chen, S. Deng, X. Jing, M. Xie, K. Ye, L. Zhang, Design and analysis of a novel three-bed series VTSA process for enhancing adsorbent utilization under low-concentration CO_2 exhaust gas conditions, Energy 320 (2025) 135388.
[9] B. Liu, T. Wang, X. Yang, P.-C. Chiang, Experimental study on energy consumption and performance of hydroxyethyl Ethylenediamine solution for CO_2 capture, Aerosol Air Qual. Res. 9 (2019) 2929–2940.
[10] F. Khaled, E. Hamad, M. Traver, C. Kalamaras, Amine-based CO_2 capture on-board of marine ships: a comparison between MEA and MDEA/PZ aqueous solvents, International Journal of Greenhouse Gas Control 135 (2024) 104168.
[11] A. Einbu, T. Pettersen, J. Morud, A. Tobiesen, C.K. Jayarathna, R. Skagestad, G. Nysæther, Energy assessments of onboard CO_2 capture from ship engines by MEA-based post combustion capture system with flue gas heat integration, International Journal of Greenhouse Gas Control 113 (2022) 103526.
[12] M. Visonà, F. Bezzo, F. d'Amore, Techno-economic analysis of onboard CO_2 capture for ultra-large container ships, Chem. Eng. J. 485 (2024) 149982.
[13] L. Shao, C. Liu, Y. Wang, Z. Yang, Z. Wu, Z. Zhao, W. Teng, D. Hu, C. Zheng, X. Gao, Reducing aerosol emissions by decoupled parameter management during the CO_2 capture process in a multi-stage circulation absorber, Environ. Sci. Technol. 57 (2023) 10467–10477.
[14] M. Xiao, W. Zheng, H. Liu, X. Luo, H. Gao, Z. Liang, Thermodynamic analysis of carbamate formation and carbon dioxide absorption in N-methylaminoethanol solution, Appl. Energy 281 (2021) 116021.
[15] Q. Luo, Q. Zhou, B. Feng, N. Li, S. Liu, A combined experimental and computational study on the shuttle mechanism of Piperazine for the enhanced CO_2 absorption in aqueous Piperazine blends, Ind. Eng. Chem. Res. 61 (2022) 1301–1312.
[16] R. Apaiyakul, P. Nimmanterdwong, T. Kanchanakungvalkul, P. Puapan, H. Gao, Z. Liang, P. Tontiwachwuthikul, T. Sema, Precipitation behavior, density, viscosity, and CO_2 absorption capacity of highly concentrated ternary AMP-PZ-MEA solvents, International Journal of Greenhouse Gas Control 120 (2022) 103775.
[17] C. Yu, H. Ling, W. Cao, F. Deng, Y. Zhao, D. Cao, M. Tie, X. Hu, Revealing the potential of cyclic amine morpholine (MOR) for CO_2 capture through a comprehensive evaluation framework and rapid screening experiments, Chem. Eng. J. 495 (2024) 153402.
[18] B. Aghel, S. Janati, S. Wongwises, M.S. Shadloo, Review on CO_2 capture by blended amine solutions, International Journal of Greenhouse Gas Control 119 (2022) 103715.
[19] R. Zhang, R. Liu, F. Barzagli, M.G. Sanku, C.e. Li, M. Xiao, CO2 absorption in blended amine solvent: speciation, equilibrium solubility and excessive property, Chem. Eng. J. 466 (2023) 143279.
[20] K. Jiang, H. Yu, L. Chen, M. Fang, M. Azzi, A. Cottrell, K. Li, An advanced, ammonia-based combined NOx/SOx/CO_2 emission control process towards a low-cost, clean coal technology, Appl. Energy 260 (2020) 114316.
[21] J. Zhou, J. Zhang, G. Jiang, K. Xie, Study on shipboard carbon capture technology with the MEA-AMP-mixed absorbent based on ship applicability perspective, ACS Omega 9 (2024) 35929–35936.
[22] X. Zhou, Y. Shen, F. Liu, J. Ye, X. Wang, J. Zhao, S. Zhang, L. Wang, S. Li, J. Chen, A novel dual-stage phase separation process for CO_2 absorption into a biphasic solvent with low energy penalty, Environ. Sci. Technol. 55 (2021) 15313–15322.
[23] Z. Huang, G. Zhan, L. Xing, B. Yuan, X. Liu, Y. Zhang, Y. Bai, Z. Chen, J. Li, Efficient dynamic phase splitting driven by centrifugal force for CO_2 capture from flue gas using biphasic solvents, Environ. Sci. Technol. 58 (2024) 16376–16385.
[24] X. Luo, M. Wang, Study of solvent-based carbon capture for cargo ships through process modelling and simulation, Appl. Energy 195 (2017) 402–413.
[25] M. Feenstra, J. Monteiro, J.T. van den Akker, M.R.M. Abu-Zahra, E. Gilling, E. Goetheer, Ship-based carbon capture onboard of diesel or LNG-fuelled ships, International Journal of Greenhouse Gas Control 85 (2019) 1–10.
[26] S. Lee, S. Yoo, H. Park, J. Ahn, D. Chang, Novel methodology for EEDI calculation considering onboard carbon capture and storage system, International Journal of Greenhouse Gas Control 105 (2021).
[27] T. Damartzis, A. Asimakopoulou, D. Koutsonikolas, G. Skevis, C. Georgopoulou, G. Dimopoulos, L. Nikolopoulos, K. Bougiouris, H. Richter, U. Lubenau, S. Economopoulos, C. Perinu, D. Hopkinson, G. Panagakos, Solvents for membrane-based post-combustion CO_2 capture for potential application in the marine environment, Appl. Sci. 12 (2022) 6100.
[28] M. Afkhamipour, M. Mofarahi, Comparison of rate-based and equilibrium-stage models of a packed column for post-combustion CO_2 capture using 2-amino-2-methyl-1-propanol (AMP) solution, International Journal of Greenhouse Gas Control 15 (2013) 186–199.
[29] W. Nguyen, S. Balchandani, B. Mandal, A. Henni, Modeling gas–liquid equilibrium of carbon dioxide in mixtures of (1-butyl-3-methyl-imidazolium acetate+1-(2-aminoethyl) piperazine+water) and (1-butyl-3-methyl-imidazolium acetate+bis (3-aminopropyl) amine+water) by electrolyte non-random two liquid (e-NRTL) model, Int. Commun. Heat Mass Transf. 154 (2024) 107393.
[30] C. Pan, C. Liu, L. Shao, F. Xu, Z. Wu, Z. Zhou, X. Zhang, Y. Zhang, C. Zheng, X. Gao, Multistage circulation absorption improvement: simulation and energy-saving evaluation of an innovative amine-based CO_2 capture process, Energy Fuel 38 (2024) 2129–2140.
[31] W. Li, Y. Zhang, Z. Zhao, C. Liu, Y. Wang, M. Shen, H. Dai, Y. Yang, C. Zheng, X. Gao, Simulation investigation on marine exhaust gas SO2 absorption by seawater scrubbing, J. Air Waste Manage. Assoc. 72 (2022) 383–402.
[32] X. Luo, M. Wang, Improving prediction accuracy of a rate-based model of an MEA-based carbon capture process for large-scale commercial deployment, Engineering 3 (2017) 232–243.
[33] Y.-M. Chen, H.-J. Hsu, Y.-J. Lin, Improving CO_2 capture efficiency with high-capacity solvents: addressing temperature-induced mass transfer limitations, Industrial & Engineering Chemistry Research 64 (2025) 2283–2293.
[34] R. Zhao, Y. Zhang, S. Zhang, Y. Li, T. Han, L. Gao, The full chain demonstration project in China—status of the CCS development in coal-fired power generation in GuoNeng Jinjie, International Journal of Greenhouse Gas Control 110 (2021) 103432.
[35] L. Liu, M. Fang, S. Xu, J. Wang, D. Guo, Development and testing of a new post-combustion CO_2 capture solvent in pilot and demonstration plant, International Journal of Greenhouse Gas Control 113 (2022) 103513.
[36] X. Chen, G. Jing, B. Lv, Z. Zhou, Reaction kinetics of CO_2 capture into AMP/PZ/DME solid-liquid biphasic solvent, J. Environ. Sci. 150 (2025) 622–631.
[37] E. Mostafavi, O. Ashrafi, P. Navarri, Assessment of process modifications for amine-based post-combustion carbon capture processes, Cleaner Engineering and Technology 4 (2021) 100249.
[38] A. Cousins, L.T. Wardhaugh, P.H.M. Feron, A survey of process flow sheet modifications for energy efficient CO_2 capture from flue gases using chemical absorption, International Journal of Greenhouse Gas Control 5 (2011) 605–619.
[39] T. Li, C. Yang, P. Tantikhajorngosol, T. Sema, Z. Liang, P. Tontiwachwuthikul, H. Liu, Comparative desorption energy consumption of post-combustion CO_2 capture integrated with mechanical vapor recompression technology, Sep. Purif. Technol. 294 (2022) 121202.
[40] C. Liu, L. Shao, C. Pan, F. Xu, Z. Wu, Z. Zhao, Y. Chen, H. Fan, C. Zheng, X. Gao, Multi-stage solvent circulation absorption enhancement: system optimization for energy-saving CO_2 capture, Sep. Purif. Technol. 332 (2024) 125644.
[41] C. Pan, L. Shao, C. Liu, Z. Zhou, Z. Zhou, S. Zhang, Q. Li, L. Deng, C. Zheng, X. Gao, Enhanced SO_2 and CO_2 synergistic capture with reduced NH_3 emissions using multi-stage solvent circulation process, Chem. Eng. J. 500 (2024) 157276.
[42] S.-Y. Oh, M. Binns, H. Cho, J.-K. Kim, Energy minimization of MEA-based CO_2 capture process, Appl. Energy 169 (2016) 353–362.